Volume 1 | Number 1 | Jan 2013 | Pages 1–100

Polymer Chemistry

www.rsc.org/polymers

ROYAL SOCIETY OF CHEMISTRY

ROYAL SOCIETY OF CHEMISTRY

www.rsc.org/polymers

Polymer Chemistry

ARTICLE

Tristable data-storage device of soluble polyimides based on novel asymmetrical diamines containing carbazole

Jing Zhao[a], Ling Peng[a], Ya-Liang Zhu[a], An-ming Zheng[b] and Ying-Zhong Shen[a*]

Two new asymmetric diamines 9-(2'-bromobenzyl)-9H-carbazole-3,6-diamine (BBCDA) and 9-[2'-(3'',4'',5''-trifluorophenyl)phenyl]-3,6-diaminocarbazole (TFDMC) were synthesised from carbazole. Tristable electrical conductivity switching and non-volatile memory effects are demonstrated in two novel soluble aromatic polyimides which were prepared from BBCDA and TFDMC by poly-condensation with Pyromelitic dianhydride (PMDA) and 2,2',3,3'-biphenyl tetracarboxylic dianhydride (BPDA) via a two-step procedure. All the three conductivity states are accessible, stable and nonerasable. It is noteworthy that the tristable phenomenon of PI-based memory devices appeared in the process of "erasing". The resulting polymers were fully characterized and they exhibited excellent organo-solubility and high thermal stability with the temperature of 5% weight loss under nitrogen atmosphere over 300 °C.

Introduction

Nowadays, polyimides have caused wide attention in the aspect of memory storage materials, because they are many charming qualities, such as high flexibility and processability, feasible manipulation of structures at the molecular scale during synthesis, etc. Carbazole as a photoconducting compound has been the subject of many studies. In addition the inherent electrodonating nature of the nitrogen atom in the conjugated aromatic rings makes it possible to form charge-transfer complexes.[1] Carbazole and its many derivatives have been covalently incorporated into polymeric systems as it can be functionalized.[2] Thus, the difunctionalizing of carbazole compounds is of practical importance, such as the application in a high-performance polyimide system. However, the solubility of many aromatic polyimides is not good, which restrains the application in polyimides-based memory devices. How to improve the solubility and processability of polyimides has been a research hotspot in the field of aromatic high polymers. These schemes could include the introduction of bulky side groups,[3,4] flexible linkages,[5,6] fluorine atoms[7,8] and unsymmetrical structures.[9-

[18] The introduction of bulky substituent into the polymer backbones is expected to enhance solubility and reduce crystallinity because of the random arrangement of substituent. In addition, the introduction of fluorine atoms into the polyimide main chains has led to new polyimides with improved melt processability and excellent optical properties. The incorporation of these groups serves to increase the free volume of the polyimides, thereby improving various properties, including the solubility and electrical insulating properties, without forfeiture of thermal stability.[3,4,15-18]

In this study, two new carbazole-containing aromatic asymmetric diamines BBCDA and TFDMC were synthesized and characterized. They were designed as promising monomers for polyimides, which were featured with high solubility and good thermal properties at the same time. Meanwhile, two functional aromatic, organo-soluble PIs bearing asymmetric carbazole moieties were also synthesized from the reactions of the two diamines with two kinds of commercial dianhydrides via a conventional two-stage process. These PIs were characterized by elemental analysis, FT-IR, ^{1}H NMR, UV-vis absorption, fluorescence spectra gel permeation chromatography (GPC), thermogravimetric analysis (TGA), differential scaning calorimetry (DSC), intrinsic viscosity measurement and cycle voltammogram (CV). Electronic switching devices were fabricated by placing the PIs-based solution-cast film between the indium-tin oxide (ITO) electrode and the Al electrode. The devices exhibited tristable electrical conductivity switching and non-volatile memory behavior. Carbazole as electron-donor, bromine atom, 3',4',5'-trifluorobiphnyl and phthalimide moieties as electron acceptor in the PIs. The electrical characteristics make these PIs potential candidates as organic tristable memory materials.

[a.] *Applied Chemistry Department, School of Material Science & Engineering, Nanjing University of Aeronautics & Astronautics, Nanjing, 210016, P. R. China. E-mail: yz_shen@nuaa.edu.cn; Fax: +86-21-52112626; Tel.: +86-25-52112906-84765*
[b.] *State Key Laboratory Magnetic Resonance and Atomatic Molecular Physics, Wuhan Centre for Magnetic Resonance, Wuhan Institute of Physics and Mathematics, Chinese Academy of Science, Wuhan 430071, P.R. China.*
† Footnotes relating to the title and/or authors should appear here.
Electronic Supplementary Information (ESI) available: FT-IR spectrum of TFDMC; FT-IR spectra of PIs; ^{1}H NMR and ^{13}C NMR spectrum of (2) and BBCDA; ^{1}H NMR spectra of PIs; DSC curves of PIs and AFM images of PIs See DOI: 10.1039/x0xx00000x
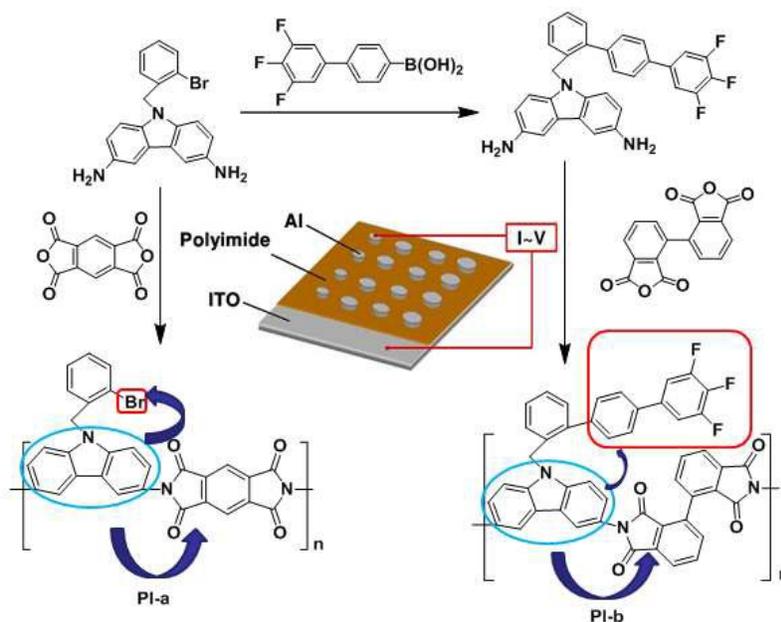
Fig. 1 Synthesis of polymers and the structure of the polyimide memory device using aluminum (Al) as top electrode and the indium-tin oxide (ITO) as bottom electrode.

Experimental

Materials

Carbazole (98%), 2-bromotoluene, 3',4',5'-trifluorobiphenyl-4-ylboronic acid (Guoyao) and Pyromelitic dianhydride (PMDA) were used as received. (Beta-4)-platinum and 2,2',3,3'-biphenyl tetracarboxylic dianhydride (BPDA) were synthesized according to the literature.[19,20] 1-bromo-2-(bromomethyl)benzene was synthesized following an already reported procedures.[21] DMF (Guoyao) was refined by reduced pressure distillation. N,N-Dimethylacetamide (DMAc, Guoyao) were distilled under reduced pressure over KOH. All the other solvents and reagents were analytical-grade and were used without further purification.

Characterization

The NMR spectra were recorded on a Bruker Advance 400 spectrometer at resonant frequencies of 400 MHz for ^{1}H and 101 MHz for ^{13}C nuclei using DMSO-d_6 as the solvent. Fourier transform infrared (FTIR) spectra of intermediates and monomer were obtained from KBr pellets with a Nicolet NEXUS-470 FTIR spectrometer. Elemental analysis was performed on a Perkine-Elmer 240C elemental analyzer. Melting points were observed in sealed capillaries with uncorrected. The weight average molecular

weight (M_w) and number average molecular weight (M_n) were determined by gel permeation chromatography (GPC) on a Water GPC system equipped with four Waters Ultrastyragel columns (300×7.5 mm, guarded and packed with 1×10^5, 1×10^4, 1×10^3, and 500 Å gels) in series. Tetrahydrofuran (THF, 1 mL min^{-1}) was used as the eluent and was monitored by a differential refractive index detector. Monodispersed polystyrene was used for the molecular weight standard. Thermo Gravimetric studie was carried out with a NETZSCH STA 449 C with a constant heating rate of 10 °C min^{-1} under nitrogen (1.0 cm^3 min^{-1}). UV-vis absorption spectra were obtained on a UV-2550 UV-vis spectrophotometer. Atomic force micrographs (AFM) with the device surface of the polymer films were obtained a NanoScope IIIa AFM operated in the tapping mode under room temperature.

Monomer synthesis

Synthesis of 3,6-Dinitrocarbazole (1). Cu(NO$_3$)$_2$·H$_2$O (5.23 g, 22 mmol) was added into a mixture of acetic acid (10 mL) and acetic anhydride (25 mL) at room temperature. The mixture was stirred for 10-20 min, and to this solution was then added carbazole (3.00 g, 18 mmol) slowly in portions over 5 min. Heat was generated during the addition (temperature rose to around 100 °C), and an additional 10 mL of acetic acid was added. The mixture was stirred at this temperature for 30 min and then poured into distilled water (200 mL). The precipitate was collected by filtration, washed with water (100 mL×3). The still wet product was then dissolved into the

ethanol solution of potassium hydroxide (KOH 25 g, water 250 mL and ethanol 250 mL). The solution turned red. After being stirred for 30 min, the solution was filtrated and the filtrate was acidified with concentrated hydrochloric acid. The yellow precipitate was then collected by filtration, washed with water and dried at 100 °C under vacuum to give yellow solid 3.94 g (85%). Mp.: 242-243 °C (DSC in air); FT-IR (KBr, cm^{-1}): 3091 (N-H stretching), 1508, 1328 (-NO$_2$ asymmetric and symmetric stretching), 860 (C-N); ^{1}H NMR (400 MHz, DMSO-d_6) δ 11.10 (s, br, 1H, NH), 9.34 (d, 2H, J = 2.3 Hz), 8.40 (dd, 2H, J = 2.3 Hz, J = 8.9 Hz), 7.78 (d, 2H, J = 8.9 Hz).

Synthesis of 9-(2-bromobenzyl)-3,6-dinitro-9H-carbazole (2). Anhydrous potassium carbonate (6.941 g, 50 mmol) and **(1)** (2.573 g, 10 mmol) which was dissolved in DMF (35 mL) were added to a 100 mL three-necked flask, and the mixture was stirred for 20 min to fully dissolved. Then 1-bromo-2-(bromethyl)benzene was added into the mixture at one time and heated at 60 °C for 4 h. After cooled to room temperature, the solution was poured into 200 mL water and collected by filtration. The solide was thoroughly washed with water, and then dried at 60 °C under vacuum to afford yellow solid 3.84 g (90% yield). Mp.: 252 °C. FT-IR (KBr, cm^{-1}): 1632 (C-C), 1521, 1331 (-NO$_2$), 1026 (C-Br). ^{1}H NMR (400 MHz, DMSO-d_6, δ, ppm): 9.61 (d, J = 2.2 Hz, 2 H, ArH), 8.44 (d, J = 2.3 Hz, 1 H, ArH), 8.42 (d, J = 2.3 Hz, 1 H, ArH), 7.83 (s, 1 H, ArH), 7.81 (s, 1 H, ArH), 7.76 (d, J = 7.9 Hz, 1 H, ArH), 7.25 (m, 1 H, ArH), 7.17 (m, 1 H, ArH), 6.41 (d, J = 7.6 Hz, 1 H, ArH), 5.91 (s, 1 H, CH$_2$). ^{13}C NMR (101 MHz, DMSO-d_6, δ, ppm): 145.3, 142.2, 135.1, 133.6, 130.2, 128.8, 127.5, 123.4, 122.9, 122.4, 119.3, 111.6, 47.9. Anal. calcd. For C$_{19}$H$_{12}$BrN$_3$O$_4$: C, 53.54; H, 2.84; N, 9.86. Found: C, 54.32; H, 2.58; N, 9.63.

Synthesis of 9-(2-bromobenzyl)-9H-carbazole-3,6-diamine (BBCDA). A three-necked flask was charged with compound **(2)** (4.26 g, 10 mmol) and 100 mL of acetic acid. The solution was stirred under a nitrogen atmosphere until **(2)** dissolved completely, and then tin powder (7.13 g, 60 mmol)、22 mL of concentrated hydrogen chloride were added. The reaction mixture was stirred at 100 °C under a nitrogen atmosphere for 30 h. After cooling, the reaction mixture were poured into sodium hydroxide solution and adjust PH to alkaline. The precipitate was collected, washed several times with water and dried at 60 °C under vacuum. After dried, the product was extracted by tetrahydrofuran and then the solvent was removed by oil pump vacuum. The residue was purified by recrystallization with ethanol and water gray solid 2.67 g (73%). Mp.: 246 °C. FT-IR (KBr, cm^{-1}): 3286 and 3196 (-NH$_2$ asymmetric and symmetric stretching), 1328 (C-N), 1026 (C-Br). ^{1}H NMR (400 MHz, DMSO-d_6, δ, ppm): 7.67 (d, J = 8.9 Hz, 1 H, ArH), 7.16 (m, 1 H, ArH), 7.14 (d, J = 2.0 Hz, 2 H, ArH), 7.09 (m, 1 H, ArH), 7.05 (s, 1 H, ArH), 7.02 (s, 1 H, ArH), 6.69 (d, J = 2.1 Hz, 1 H, ArH), 6.67 (d, J = 2.1 Hz, 1 H, ArH), 6.25 (d, J = 7.6 Hz, 1 H, ArH), 5.41 (s, 2 H, CH$_2$), 4.67 (s, 4 H, NH$_2$). ^{13}C NMR (101 MHz, DMSO-d_6, δ, ppm): 141.6, 137.5, 134.3, 133.1, 129.5, 128.3, 123.2, 122.1, 115.4, 109.7, 104.6, 46.5. MS (ESI, m/z): 365.00 ([M-H]$^-$, calcd for C$_{19}$H$_{16}$BrN$_3$, 366.25). Anal. calcd. For C$_{19}$H$_{12}$BrN$_3$O$_4$: C, 53.54; H, 2.84; N, 9.86. Found: C, 54.32; H, 2.58; N, 9.63.

Synthesis of 9-[-2'-(3'',4'',5''-trifluorophenyl)phenyl]-3,6-diaminocarbazole (TFDMC). To a 100 mL three-necked round-bottomed flask, a mixture of **BBDCA** (1.0 g, 2.74 mmol), 3',4',5'-trifluorobiphenyl-4-ylboronic acid (0.89 g, 3.56 mmol), Pd(PPh$_3$)$_4$ (0.033 g, 0.028 mmol), Na$_2$CO$_3$ (0.60 g, 5.64 mmol), toluene (22 mL) and water (11 mL) was added and the reaction mixture was heated at 100 °C under a nitrogen atmosphere for 6 h. When the reaction was completed, the reaction mixture was cooled to room temperature and filtered. The crude product was achieved by extraction with toluene. After remove solvent, the crude product was recrystallized from ethanol and water to afford 1.12 g (83%). Mp.: 196 °C. FT-IR (KBr, cm^{-1}): 3435、3346 (-NH$_2$), 1324 (C-N), 1201、834 (C-F). ^{1}H NMR (400 MHz, DMSO-d_6, δ, ppm): 7.9 (d, J = 8.2 Hz, 2 H, ArH), 7.85-7.76 (m, 2 H, ArH), 7.70 (s, 1 H, ArH), 7.68 (s, 1 H, ArH), 7.37-7.25 (m, 2 H, ArH), 7.12 (d, J = 9.3 Hz, 2 H, ArH), 6.92 (s, 1 H, ArH), 6.90 (s, 1 H, ArH), 6.65 (d, J = 10.4 Hz, 2 H, ArH), 6.47 (d, J = 7.8 Hz, 1 H, ArH), 5.36 (s, 2 H, CH$_2$), 4.62 (s, 4 H, NH$_2$). ^{13}C NMR (101 MHz, DMSO-d_6, δ, ppm): 141.4, 140.8, 140.1, 136.4, 136.0, 134.4, 130.3, 130.2, 128.2, 127.5, 127.4, 126.3, 123.1, 115.2, 111.9, 111.8, 111.7, 111.6, 109.5, 104.5, 44.4. MS (ESI, m/z): 494.50 ([M+H]$^+$, calcd for C$_{31}$H$_{22}$F$_3$N$_3$, 493.52). Anal. calcd. For C$_{31}$H$_{22}$F$_3$N$_3$: C, 75.44, H, 4.49, N, 8.51. Found: C, 75.41, H, 4.50, N, 8.54.

Polymer synthesis

All polymers were synthesized via a two-step procedure. In detail, taking the preparation of PI-**a** as an example, PMDA (0.61 g, 2 mmol) was added into a solution of BBDCA (0.73 g, 2 mmol) in dehydrated DMAc under nitrogen. The mixture was stirred at room temperature for 24 h to form the solution of poly(amic acid). A mixture of equimolar acetic anhydride and pyridine was added to the poly(amic acid) solution with stirring at room temperature for 2 h, and it was then heated to 100 °C for 6 h. After the reaction was completed, the mixture was cooled to room temperature. The viscous solution of polymer was poured into methanol and collected by filtration. The resulting polyimide was thoroughly washed with methanol and water, and then dried at 60 °C under vacuum for 12 h.

The yield of PI-**a** was 91%. The number average molecular weight (M_n) and weight average molecular weight (M_w) values tested by GPC were 19,500 and 29,800, respectively, with the dispersity (PDI = M_w/M_n) at 1.52; FTIR: (KBr, cm^{-1}) 1771 and 1720 (C=O asymmetric and symmetric stretching), 1486, 1371 (C-N), 1029 (C-Br). Anal. calcd. for (C$_{31}$H$_{20}$N$_3$O$_4$Br)$_n$: C, 64.37; H, 3.49; N, 7.26; Found: C, 64.69; H, 3.34; N,7.59.

The yield of PI-**b** was 89%. The number average molecular weight (M_n) and weight average molecular weight (M_w) values tested by GPC were 17,400 and 28,300, respectively, with the dispersity (PDI = M_w/M_n) at 1.62. FTIR: (KBr, cm^{-1}) 1771 and 1720 (C=O), 1593, 1441 (C-N), 1041 (C-F). Anal. calcd. for (C$_{49}$H$_{30}$F$_3$N$_3$O$_4$)$_n$: C, 75.28; H, 3.87; N, 7.29; Found: C, 74.96; H, 3.93; N, 7.52.

### Device Fabrication and Characterization

The indium-tin oxide (ITO, around 200 nm in thickness) coated onto glass substrate was used as a bottom electrode. Ahead of coating of the polymer film, the glass surfaces were cleaned with deionized

water, isopropanol and acetone by ultrasonication for 30 min, respectively. Then a solution of polyimide (16 mg/mL) filtered through polytetrafluoroethylene (PTFE) membrane syringe filters with a pore size of 0.22 mm which was spin-coated onto the ITO substrate at a revolving speed of 1800 rpm for 1 min, and residual solvent was removed under a vacuum at 60 °C for 24 h.[22] The thickness of polymer films was determined to be around 20 nm. Finally, the thickness of Al top electrodes about 110 nm was formed by thermal evaporation onto the polymer surface through a shadow mask at a pressure of about 10^{-6} Torr with a uniform depositing rate of 1-2 Å/s. Every electrical measurement of the devices was characterized under ambient conditions, without any encapsulation, using an Agilent B1500A semiconductor analyzer. During the electrical measurements, ITO was maintained as the ground electrode (the cathode). During the voltage sweep, Al was set as the top electrode (the anode) as shown Fig. 1.

Results and discussion

Monomer synthesis

A novel asymmetric carbazole-based dimine was synthesized by Suzuki coupling reaction with the high yield of 83% (Scheme 1), which contains 3',4',5'-trifluorobiphenyl moieties. In FT-IR spectrum (ESI, Figure S1), 3420 and 3338 cm^{-1} were the characteristic absorption of N–H asymmetric stretching and symmetric stretching and the C-F characteristic absorption located at 1048 cm^{-1}. ^{1}H and ^{13}C NMR spectra of TFDMC are shown in Fig. 2 with the assignment of the observed resonance. All the spectroscopic data were in good agreement with the expected structure.
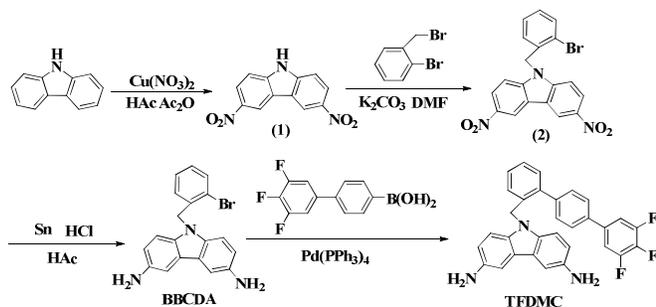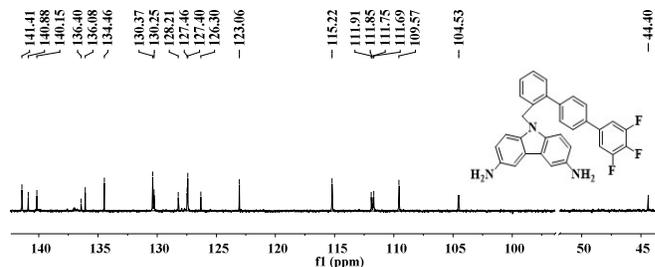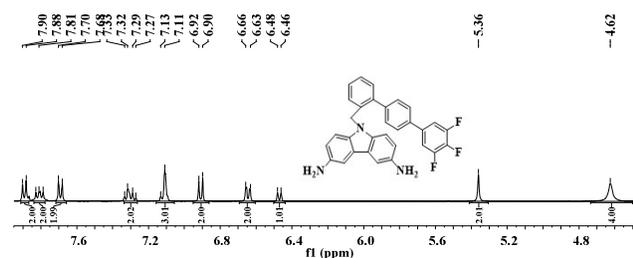

Scheme 1 Synthesis of diamines.

Fig. 2 ^{1}H NMR and ^{13}C NMR spectra of TFDMC.

Polyimides synthesis

The functional polyimides PI-**a** and PI-**b** were prepared from the new diamines (BBCDA, TFDMC) with the respective aromatic dianhydrides (PMDA, BPDA) via a two-step poly-condensation method (Fig. 1). In this procedure, the first step was to form the poly(amic-acid)s at room temperature (r.t.). Then, a dehydrating agent, such as a mixture of acetic anhydride and pyridine was added into the system, formed effective chemical imidization to obtain the polyimides. The FTIR spectra of polymers confirmed effective formation of polyimides as shown in Figure S2 (ESI). The characteristic bands at 1777 and 1714 cm^{-1} are attributed to the asymmetric and symmetric stretching of imide carbonyl groups, respectively, and a band at 1371 cm^{-1} due to C-N stretching vibration which confirmed the formation of imide structure. In addition, the characteristic absorption of the C-F group located at about 1041 and 1111 cm^{-1} can also be observed. The chemical structures of the PIs were also verified by ^{1}H NMR spectroscopy. ^{1}H NMR spectra of PIs are shown in Figure S7 (ESI), the complete disappearances of the amino proton signal at 4-5 ppm provide confirmation of the diamines were fully polymerized in the first step. However, from these spectra, the appearances -NH-CO- and –COOH proton weak signal at 10-11 ppm illustrated that a small amount of acid without cyclization completely in the second step of polymerization process. In general, the result shows that the spectroscopic data were in good agreement with the expected structure. The elemental analysis results of C, H and N content are in a fair agreement with the theoretical content. The FTIR ^{1}H NMR and elemental analysis suggest the successful preparation of the target polyimides.

Organo-solubility and thermal properties of polymers

The inherent viscosities and solubility of the synthesized PIs in common solvents are summarized in Table 1. These polymers exhibited good solubility in various solvents such as DMAc, N-methylpyrrolidone (NMP), N,N-dimethylformamide (DMF), THF, CHCl₃, toluene and acetone at room temperature or upon heating at 80 °C. The PIs demonstrated moderate to high inherent viscosities of PI-a and PI-b were of 0.65 and 0.63 dL/g, respectively. Apparently, the solubility of PI-**b** is better than PI-**a**, this can be attributed to the structural modification through the incorporation of the bulky and non-coplanar units in the side chain,[23] which renders the polymer non-coplanar and also reduces inter-chain

interactions. These PIs were investigated by X-ray powder diffraction. From all these diffraction patterns (Fig. 3), it was observed that all the PIs displayed a typical amorphous pattern and not able to show any crystallinity. This property provides good quality thin film by means of a conventional solution spin-casting process. Obviously, the amorphous nature of the asymmetry aromatic-substituted carbazole-based polyimides was also reflected in their good dissolvability.[24] The thermal properties of the polyimides were evaluated by TGA (Fig. 4) and DSC (ESI, Figure S8) in the atmosphere of nitrogen. The 10% weight-loss temperature of PI-a and PI-b were 388 °C and 413 °C, respectively. The anaerobic char yield of these polymers in nitrogen was about 40% at 800 °C. The high char yields can be ascribed to the high aromatic content in

these polymers. From the DSC curves, the PI-a and PI-b showed the glass transition temperature at 321 °C and 301 °C, respectively. The lower T_g of PI-b compared to PI-a could be attributed to the introduction of bulky side-chain substituted group of 3',4',5'-trifluorobiphenyl in TFDMC and PI-b. The introduction of non-coplanar bulky aromatic side group at the 9-position in the carbazole structure aggrandize the size and sharp anisotropy of the diamine with 9-substituted aryl group, which in turn affects the molecular packing. As a result, the machinability of these relatively intractable polymers is improved. These results show that the new-synthesized ployimides are thermally stable and dimensionally polymers, which is required to be used in the electronics industry from the heat resistance point of view.

Table 1 The inherent viscosity and solubility of PIs.

Sample	η_{inh} (dL/g)	DMAc	DMF	NMP	THF	CHCl$_3$	丙酮	甲苯
PI-a	0.65	+++	+++	++	+	+	-	-
PI-b	0.63	+++	+++	+++	+++	++	+	+

η_{inh}, intrinsic viscosity measured at a concentration of 0.5 g·dL^{-1} in DMAc at 30 °C; +++, soluble at room temperature; ++, soluble on heating; +, slightly soluble on heating; -, insoluble even on heating.
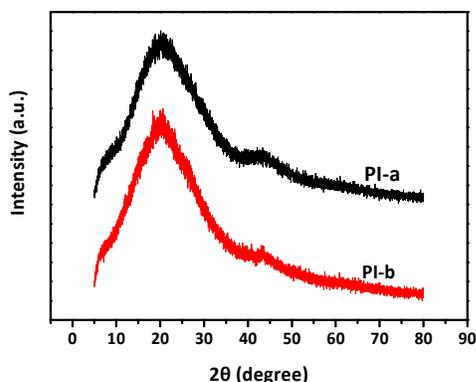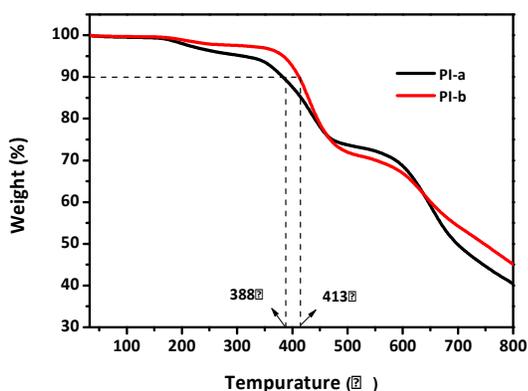

Fig. 3 Diffraction patterns of PIs.

Fig. 4 TGA curves of PIs under nitrogen atmosphere at a heating rate of 10.0 °C ·min^{-1}.

Atomic Force Microscope (AFM) morphology of the polymer films

AFM was used to characterize the surface morphologies and roughness of polymer films. The morphology of the polymer films plays an important role in determining the device performance. As shown in Figure S9 (ESI), the three-dimensional images of different polyimides. The thick of polymer films are about 20 nm evaluated by AFM, the RMS (root-mean-square) roughness ranges from 1.537 to 2.25 nm, demonstrating the excellent ability of film-forming for these polyimides.

Optical and electrochemical properties

UV-vis absorption spectra and photoluminescence (PL) of the PIs in THF solution are shown in Fig. 5. The UV-vis spectrum of PI-**a** and PI-**b** show the absorption peak maximum(λ_{max}) at 232 and 239 nm, which could be attributed to the introduction of asymmetric groups make the molecules are not coplanar and reduce the conjugate degree. The emission peaks of PI-**a** and PI-**b** were observed at 373 and 341 nm when they were excited at the maximum absorption wavelength. The higher fluorescence intensity of PI-**b** compared to PI-a could be attributed to more aromatic rings in TFDMC. Moreover, the optical band gap (Eopt) of the PIs are estimated to be 3.87 and 3.85 eV. Fig. 6 shows the cyclic voltammograms (CVs) of the PIs on platinum electrode in 0.1 M acetonitrile solution of tetrabutylammonium hexauorophosphate. The oxidation halfwaves potentials ($E_{1/2}$) for PIs were determined to be 1.87 and 2.08 vs. Hg/Hg$_2$Cl$_2$, respectively. The external ferrocene ferrocenium (Fc/Fc$^+$) redox standard potential, $E_{1/2}$, was measured to be 0.49 V vs. Hg/Hg$_2$Cl$_2$ in acetonitrile. Assuming that the HOMO level for the Fc/Fc$^+$ standard is -4.8 eV with respect to the zero vacuum level, the HOMO levels for PI-**a** and PI-**b** are determined to be -6.18 and -6.39

eV. Therefore，the LUMO levels of the two PIs are estimated to be -2.31 and -2.54 eV. This result indicates that PI-**a** could provide more stable and lower HOMO energy level. In the Al/PI-**a**/ITO device, the energy barrier to hole injection from electrode to the active layer was estimated to be 1.38 eV from the work function (Φ) of ITO (-4.80 eV) and the HOMO of the active PI layer, and the energy barrier to electron injection from the electrode to the active layer was estimated to be 1.97 eV from the Φ of Al (-4.28 eV) and the LUMO of the active layer. This shows that hole injection from ITO into the HOMO of PI-**a** is easier than electron injection from Al into the LUMO of PI-**a**. As a result, PI-**a** is a p-type material, and the PI-**b** also display the similar p-type material properties.
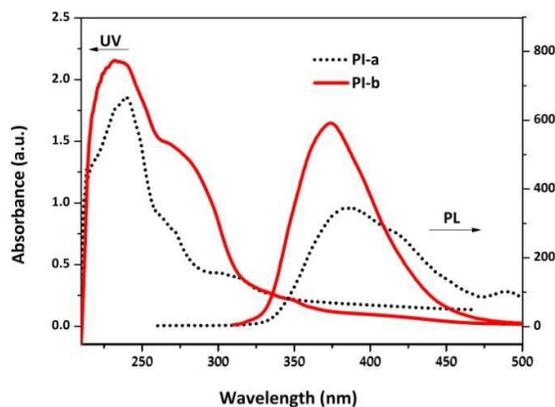

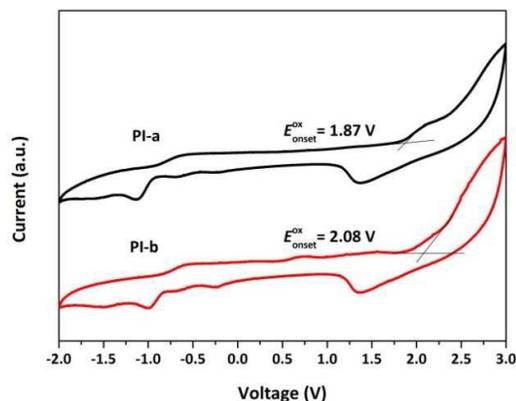Fig. 5 UV-vis and photoluminescence spectra of PI-**a** and PI-**b** THF solution.

Fig. 6 CV responses of PI-**a** and PI-**b** films coated ITO electrodes in 0.1 M n-Bu₄NClO₄/acetonitrile solution with a platinum plate counter electrode and an Ag/AgCl (3.8 M KCl) reference electrode. A scan rate of 50 mV/s was used.

Electrical characteristics of the PI-based memory devices

The memory behaviors and electrical switching of the PIs was tested by the current-voltage (I-V) measurements of an Al/polymer/ITO sandwich device.[20-23] The I-V curves reveal tristable conductivity switching. The typical I-V characteristics of the Al/PI-**a**/ITO memory devices in semilog scale of the devices are shown in Fig. 7a. Initially, the as-fabricated device was in the low-conductivity (OFF) state. During the first negative sweep from 0 to -5 V, the current remained low until the switching threshold voltage of -3.9 V was reached. At the voltage, the current sharp increased from 10^{-6} to 10^{-3}, indicating the device transition from initial OFF state to the high-conductivity (ON) state, which serves as the "writing" process for the memory device. After the transition, the device remained in the ON-state even after bias interruption. As the applied voltage exceeds +1.9 V, an abrupt decrease in current from 10^{-2} to 10^{-5}, which indicates the device transition to the first low-conductivity (OFF-1) state. Subsequent positive sweep (sweep 4) show that the device remains in the OFF-1 state. When the voltage increases to +4.8 V, the device switches form the OFF-1 state to the OFF-2 (second low-conductivity) state. The transition from the on state to the OFF-1 state or from the OFF-1 state to the OFF-2 state serves as an "erasing" process for the memory device. Moreover, this type of OFF-state can be maintained during the sweep 5 and after the power is turned off. These results indicate that the devices are nonvolatile memory and possess the ability of writing, reading, and erasing cycles to meet the requirement of a flash memory device. Further, the retention characteristic of the ON/OFF states for Al/PI-**a**/ITO sandwich device is shown in Fig. 7b. No degradation was observed during the test.
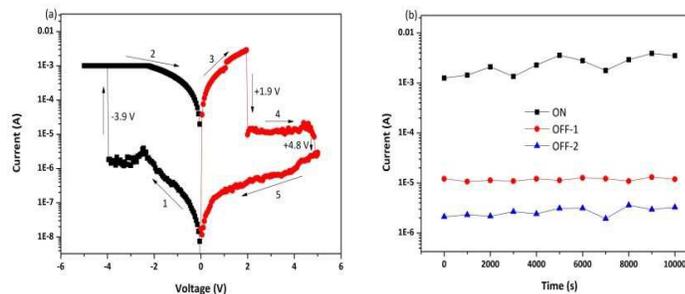

Fig. 7 (a) I-V characteristics of Al/PI-a/ITO device with an electrode area of 0.0314 mm². (b) Effect of operation time on the ON and OFF states of the Al/PI-**a**/ITO device under a constant stress of 0.5 V at room temperature.
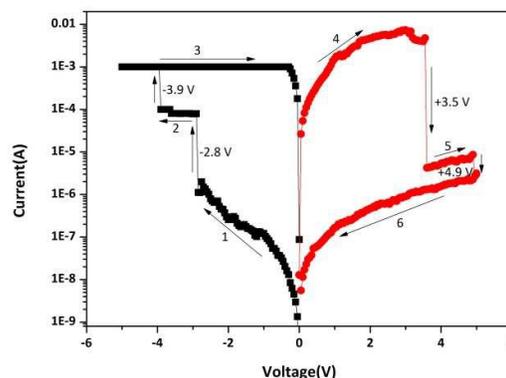

Fig. 8 I-V characteristics of Al/PI-**b**/ITO device with an electrode area of 0.0314 mm².

Fig 8 exhibits the typical I-V characteristic of the memory device fabricated with the PI-**b** film. During voltage sweeping from 0 to -5.0 V, the current remains low until the switching voltage of -2.8 V is reached. I increases abruptly from 10^{-6} to 10^{-4} A at -2.8 V, indicating device transition to the first high-conductivity (ON-1) state. Subsequent negative sweep show that the device remains in the ON-1 state. As the applied voltage exceeds -3.9 V, the current increases abruptly again from 10^{-4} to 10^{-3} A, switching the device from the ON-1 state to the second high-conductivity (ON-2) state. The transition from the OFF state to the ON-1 state or from the ON-1 state to the ON-2 state serves as a "writing" process for the memory device. The device remains in the ON-2 state under both the negative (sweep 3) and positive voltage scans (sweep 4). However, the current decreases abruptly from 10^{-2} to 10^{-5} when the voltage is increased up to +3.5 V, indicating the device transition to the first low-conductivity (OFF-1) state. Subsequent positive sweep show that the device remains in the OFF-1 state. When the voltage increases to +4.9 V, the device switches form the OFF-1 state to the OFF-2 (second low-conductivity) state. The transition from the ON state to the OFF-1 state or from the OFF-1 state to the OFF-2 state serves as an "erasing" process for the memory device. The I–V characteristic, therefore, indicate that the device behaves as a Flash memory. However, the retention characteristic of the ON/OFF states for Al/PI-**a**/ITO sandwich device is not very satisfactory.

Electrical switching mechanism of the memory devices

To obtain the switching mechanism of memory devices based on the PIs layer, the electronic characteristics were studied by I–V properties of ON- and OFF-state. The introduction of electron-withdrawing unit, such as fluorine and oxygen atom, is expected to lower the LUMO level in poly-conjugated systems facilitating the electron injection.[25] In particular, the HOMO represents electron density localization for an electron donor in the ground state, while LUMO stands for the electron density localization in the excited state. The LUMO energy level of the donor must have a proper match with that of the acceptor to offer enough driving force for charge separation.[26] The lower HOMO energy levels of PIs, the higher turn-on threshold voltage. The turn-on voltage of the PIs is PI-**a** > PI-**b**, and these PIs are in agreement with the ordering of HOMO energy levels estimated by the CV measurement. The different electron donor or acceptor substituents on the conjugated systems could change the aromaticity and the steric hindrance in polymeric systems. Just as PI-**b**, the substituted group in 2'-position of the aryl is electron acceptor. Further detailed information about the switching mechanism of the PIs is supported by the field-induced CT effect form the theoretical calculation as described below.[27,28] Molecular simulations, on the basic unit (BU) of PI-**a** and PI-**b** were carried out by density functional theory (DFT) theoretical calculations. Calculations of the molecular orbitals and optimized geometry of the BU were carried out at the WB97XD/6-31G(D, P) level with the Gaussian 03 program package,[29] and then the molecular orbital of HOMOs and LUMOs were predicted at the same level. Electric density contours and the corresponding energy levels are presented in Fig. 9, respectively. The calculated energy levels (HOMO, LUMO)

of PI-**a** and PI-**b** were of (-6.43, -2.35) and (-6.35, -2.13) eV, respectively, which are consistent with those determined from the CV measurement ((HOMO, LUMO) energy levels of (-6.18, -2.31) and (-6.39, -2.54) eV, respectively. The HOMOs of the PIs are mainly on the carbazole part, the carbazole moieties are the main electron donors and bromine atom, 3',4',5'-trifluorobiphnyl, phthalimide moieties are the electron acceptors. For the BU of PI-a, the HOMO is located on carbazole of the amine parts. The LUMO is distributed on anhydride unit. The electronic transition corresponds to promotion of an electron at the excited state. The energy barrier for hole injection from work function of ITO to the HOMO of the active layer is lower than the energy barriers between the work function of Al and HOMO. Therefore, hole injection is a favored process under a negative bias.
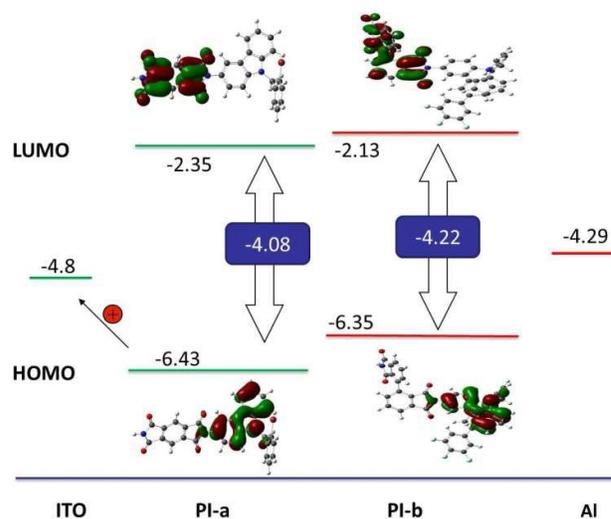

Fig. 9 LUMO and HOMO energy levels for the two molecules, calculation based on DFT.

The positive and negative charges are segregated from the CT process and localized in the donor and acceptor under the electric bias. The increasing numbers of migrating carriers result in the open pathway with the high conductance of memory device. In the device of PI-**b**, there was energy barrier which could block the electron migration between the donor (carbazole group) and acceptor-1 (3',4',5'-trifluorobiphnyl), once an electric field was applied, the shallow charge traps in acceptor-1 was filled progressively, the device was switched from the OFF to the ON-1 state. Increasing the applied electric field, the traps arising from the acceptor-2 (dianhydrides) unit were filled sequentially, corresponding to the current transition from the ON-1 to the ON-2 state. As the electron withdrawing ability of bromine atom in PI-**a** is weak, it couldn't show obvious ternary state in the process of "writing". When in the process of "erasing", the devices of PI-**a** and PI-**b** exhibited the similar tristable phenomenon which was attributed to the asymmetrical substituted groups in 9-position made electron delocalization is

limited. The polymers could restored to the initial structure under reverse electric field.

Conclusion

We have successfully synthesized two novel asymmetry diamines having aryl group on 9-position of carbazole, which was synthesized from 9-(2-bromobenzyl)-3,6-diaminocarbazole reacting with corresponding arylbronic acids via Suzuki coupling reaction. All of new compounds were confirmed by spectroscopic means, two functional soluble PIs were prepared by condensation reaction with two type dianhydrides in DMAc, and through chemical imidization. Finally, we got two novel PIs, and all PIs exhibited excellent solubility and thermal stability. The storage devices with a configuration of ITO/PI/Al showed similar switching characteristics which were found to be varied continuously. Memory devices with the PIs films exhibited bipolar ternary flash type memory characteristics with low switching voltage less than 5 V. In additional, the ON/OFF current ratios of 10^3-10^4 are observed in all memory devices and long retention times of 10^4 s even in ambient atmosphere. This present study suggests that these novel PIs with containing cabazole have potential applications for organic multilevel data devices.

Acknowledgements

References

1   T. Wada, and H. Sasabe, Polym. Prepr(Div. Polym. Chem)., 1993, 34, 763.
2   J. P. Chen, A. Natansohn, *Macromolecules,* 1999, **32**, 3172.
3   A. L. Rusanor, Z. B. shirina, *High Perform. Polym*, 1993, **5**, 107.
4   F. W. Harris, Y. Sakaguchi andM. Shibata, *High Perform. Polym*., 1997, **9**, 251.
5   S. H. Hsiao, H. M. Wang and J. S. Chou, *J. Polym. Res.*, 2012, **19** article NO. 9757.
6   P. Thiruvasagam and M. Vijayan, *J. Polym. Res.,* 2012, **19** article NO. 9845.
7   C. L. Chung, T. W. Tzu and S. H. Hsiao, *J. Polym. Res.,* 2006, **13**, 495.
8   C. P. Yang, Y.C. Chen and S.H. Hsiao, *J. Polym. Res.,* 2010, **17**, 779.
9   X. Z. Fang, Z. Wang and Z. H. Yang, *Polymer,* 2003, **44**, 2641.
10 J. W. Xu, M. L. Chang and T. S. Chung, *Polymer*, 2003, **44**, 4715.
11 C. P. Yang and Y. Y. Su, *Polymer,* 2003, **44**, 6311.
12 X. Z. Fang, Z. H. Yang and L. X. Guo, *Polymer,* 2004, **45**, 2539.
13 C. P. Yang , Y. Y. Su and K. L. Wu, *J Polym Sci Polym Chem*, 2004, **42**, 5424.
14 M. Zhang, Z. Wang and M. X. Ding, *J Polym Sci Polym Chem,* 2006, **44**, 959.
15 I. S. Chung and Y .K. Sang, *Macromolecules*, 2000, **33**, 3190.
16 S. D. Kim, S. Lee and I. S. Chung, *Polymer*, 2013, **54**, 5648.
17 S. D. Kim, S. Y. Kim and I. S. Chung, *J. Polym. Sci. Part A Polym. Chem.*, 2013, **51**, 4413.
18 S. D. Kim, S. Y. Kim and I. S. Chung, *Macromolecules*, 2014, **47**, 8846.
19 K. L. Wang, W. T. Liou and S. T. Huang, *Polymer*, 2008, **49**, 1538.
20 C. Laurent, E. Kay and N. J. Souag, *Appl Phys.*, 1988, **64**, 336.
21 L. Li, Q. D. Ling and D. S. Chan, Org Electron., 2007, **8**, 401.
22 K. L. Jensen, *J Vac Sci Technol.*, 2003, **21**, 1528.
23 Q. D. Ling, W. Wang and E. T. Kang, *J Phys Chem B.*, 2006, **110**, 3995.
24 Y. Q. Li, H. H. Xu and Y. Z. Shen, *J. Mater. Chem.*, 2011, **21**, 1810.
25 F. Babudri, G. M. Farinola and R. Ragni. *Chem Commun.,* 2007, **10**, 1003.
26 N. H. You, C. C. Chueh and W. C. Chen, *Macromolecules*, 2009, 42, 4456.
27 S. L. Lim, T. E. Ling and D. S. Chan, *Chem Mater*, 2007, **19**, 5148.
28 J. Hu, Y. Li and W. Hu, *J Mater Chem.,* 2007, **17**, 3530.
29 M. J. Frisch, G. W. Trucks and J. R. Cheeseman, Gaussian 09, (Revision B.01). Wallingford CT: Gaussian Inc.; 2010.

For Table of Contents Use Only

Tristable data-storage device of soluble polyimides based on novel asymmetrical diamines containing carbazole

Jing Zhao[a], Ling Peng[a], Ya-Liang Zhu[a], An-ming Zheng[b] and Ying-Zhong Shen[a*]

Two novel soluble aromatic polyimides were prepared from BBCDA and TFDMC by poly-condensation with Pyromelitic dianhydride (PMDA) and 2,2′,3,3′-biphenyl tetracarboxylic dianhydride (BPDA) via a two-step procedure. Memory devices fabricated with PIs as shown Fig. 1. In the device, ITO was maintained as the ground electrode (the cathode) and Al was set as the top electrode (the anode).
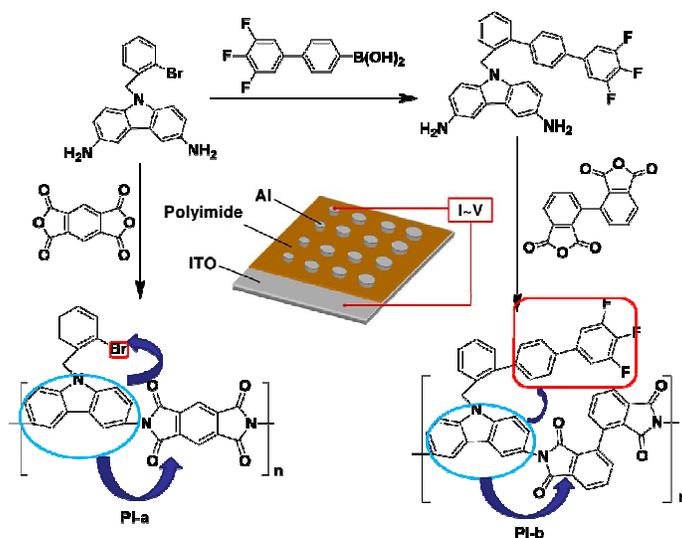

Fig. 1

The PI-based device exhibited bipolar ternary flash type memory characteristic. It is noteworthy that the tristable phenomenon of PI-based memory devices appeared in the process of "erasing".
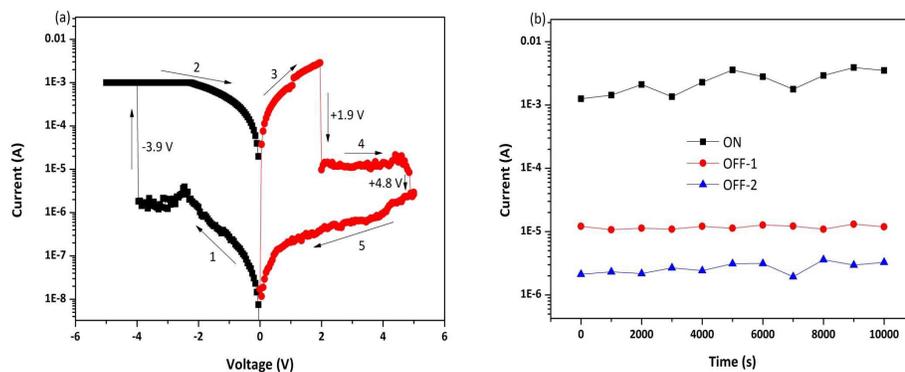

Fig. 2